Biomechanical and Physiological Evaluation of Biologically-Inspired Hip Assistance With Belt-Type Soft Exosuits

Qiang Chen, Shijie Guo, *Member, IEEE*, Jing Wang, Jiaxin Wang, Dan Zhang, *Senior Member, IEEE*, and Shanhai Jin, *Member, IEEE*

***Abstract*— Hip-assisted soft exosuits have been reported for their effect on reducing the metabolic power of human walking. Currently, most studies focus on uni-directional assistance (HF: hip flexion, or HE: hip extension). This paper investigates the effect of bi-directional assistance (HFE: hip flexion and extension) on the biomechanics and physiology of the wearer for understanding the potential benefits in synergistic effect of multi-muscle assistance. A belt-type soft exosuit was developed to provide the bi-directional assistance for augmenting walking. The assistance strategy was presented by imitating the contraction mechanisms of hip flexor and extensor muscles in walking. Tests on 8 healthy subjects were conducted and the results were compared with traditional uni-directional assistance. Metabolic powers, muscle activities, kinematics, and kinetics were measured and analyzed. Results showed that HFE assistance reduced the metabolic power by 7% and 12.4% relative to no exosuit and assistance turned off, respectively, larger than the sum of HF and HE. Furthermore, HFE reduced more total joint positive biological work and the activity of more related muscles, and at the same time increased upward and downward accelerations of body mass center, promoting walking energy exchange. These findings demonstrate that bi-directional assistance by combining hip flexion and extension has a significant synergistic effect on augmenting human walking as well as a benefit of increasing biological efficiency.**

Manuscript received 19 March 2022; revised 16 July 2022 and 6 September 2022; accepted 18 September 2022. Date of publication 26 September 2022; date of current version 7 October 2022. This work was supported by the Major Project of New Generation AI of Tianjin under Grant 18ZXZNSY00270. *(Corresponding author: Shijie Guo.)*

This work involved human subjects or animals in its research. Approval of all ethical and experimental procedures and protocols was granted by the Biomedical Ethics Committee, Hebei University of Technology, Tianjin, China.

Qiang Chen and Shijie Guo are with the State Key Laboratory of Reliability and Intelligence of Electrical Equipment, Hebei Key Laboratory of Robot Sensing and Human–Robot Interaction, School of Mechanical Engineering, Hebei University of Technology, Tianjin 300401, China (e-mail: guoshijie@hebut.edu.cn).

Jing Wang is with the Key Laboratory of Exercise Physiology and Sports Medicine, Tianjin University of Sport, Tianjin 301617, China.

Jiaxin Wang is with the School of Mechanical Engineering, Hebei University of Technology, Tianjin 300401, China.

Dan Zhang is with the Department of Mechanical Engineering, York University, Toronto, ON M3J 1P3, Canada.

Shanhai Jin is with the School of Engineering, Yanbian University, Yanji 133002, China.

Digital Object Identifier 10.1109/TNSRE.2022.3209337

***Index Terms*— Soft exosuit, hip assistance, muscle contraction, metabolic power, synergistic effect.**

I. Introduction

LOWER limbs act as struts of an inverted pendulum to move the body forward during human walking, and the movement is continued by the transition from one pendulum-like stance leg to the next [1]. The hip joint has an important effect on this smooth transition. Hip extension promotes the stance leg to raise center of body mass (COM). Hip flexion promotes the motion of the swing leg in preparation for receiving the energy of the stance leg, and taking on the role of next stance leg [2], [3], [4]. In the process, hip flexor and extensor muscles generate a large amount of biological work, thus leading to significant metabolic power expenditure [5], [6], [7]. Studies showed that hip torque actuation can reduce the energy cost and improve the stability of walking [8], [9].

A variety of powered hip exoskeletons have been developed for augmenting walking, or improving gait function [10], [11]. They are classified into two categories: rigid type and soft type. The rigid type can supply a powerful torque to the wearer's joint via direct or indirect motor drive [12], [13], [14]. However, the rigid nature presents some challenges because the motor and its accompanying rigid components may produce a constraint to the natural motion of the wearer, resulting in an extra metabolic increase [15], [16]. Soft exoskeletons, also called "exosuits", have attracted an extensive attention due to their light weight, easy to put on and off, and not restricting the free motion of the wearer and so on. It compensates for some limitations of rigid exoskeletons [17]. The soft components of the exosuits are attached on the body surface as anchors, and the assistive force between the anchors is transmitted by a flexible Bowden cables or soft belts [18], [19], [20].

Ding *et al.* [20] and Lee *et al.* [21] developed soft exosuits powered by an off-board tethered actuation platform that can provide hip extension (HE) assistance, and reported a 4.6% metabolic reduction for walking and a 9.1% reduction for running, respectively, relative to the results with assistance turned off. Kim *et al.* [22] presented a portable exosuit for HE assistance during outdoor walking. A 9.3% metabolic reduction was reported compared to the walking without

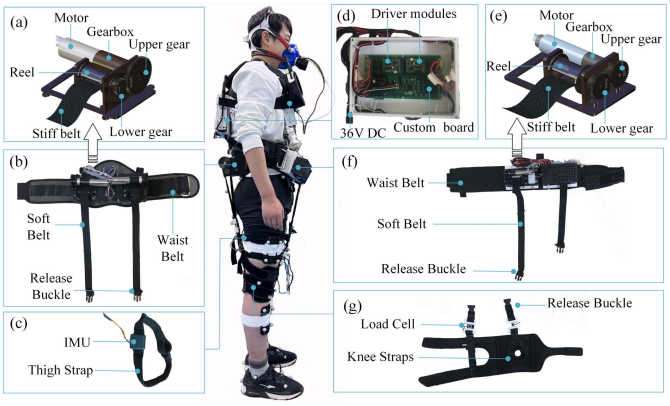

Fig. 1. Belt-type soft exosuit. (a) Extension actuator. (b) Extension unit. (c) IMU. (d) Control box. (e) Flexion actuator. (f) Flexion unit. (g) Knee strap.

wearing exosuit. Jin *et al.* [18] developed a belt-type soft exosuit to provide hip flexion (HF) assistance, and reported a 5.9% metabolic reduction relative to the results with assistance turned off. A study by Guo *et al.* [23] showed that HF assistance can improve the gait function of the elderly. Studies cited above demonstrated the effects of uni-directional hip assistance on the metabolic reduction. However, the bi-directional synergy of hip flexor and extensor muscles is crucial to human walking [24], [25].

Recently, a few studies have been conducted to investigate the effect of hip bi-directional assistance (HFE: hip flexion and extension), reported reductions in metabolic power [26] and muscle activities of hip flexors and extensors [27]. Previously, we developed a soft exosuit for HFE assistance for younger individuals during loaded walking [28], An 8.53 $\pm$ 2.65% metabolic reduction was reported relative to assistance turned off. Currently, few studies are proposed for the design of hip assistance from the muscle functional level and a comprehensive evaluation on the biomechanics and physiology of the wearer is necessary for the HFE assistance to understand its effect of multi-muscle assistance.

In this study, a belt-type soft exosuit with a simpler structure and lighter weight was developed to provide HFE assistance for augmenting human walking (Fig. 1). Inspired by the contraction mechanisms of the hip flexor and extensor muscles, a more rational strategy for HFE assistance was designed. Specifically, the force profiles for hip flexion and extension assistance were defined by customized functions, and were configured to approximate that of the muscle forces of hip flexors and extensors. Additionally, the assistive forces were optimized based on the gait information measured using IMUs attached on thighs. A zero-crossing point of hip angular velocity, as an accurate kinematic feature at the start of hip biological positive power, were used to trigger the positive power assistance, which was based on the knowledge that concentric muscle work is metabolically more expensive [29]. The HFE assistance was compared with the two uni-directional assistances (HF and HE) by walking tests on eight subjects. The metabolic powers, muscle activities, kinematics, and kinetics were measured and analyzed for understanding the underlying mechanics of metabolic reduction for each assistance mode. Experiment result demonstrated the advantage of the synergistic effect of multi-muscle assistance provided by HFE.

II. Exosuit Design

The exosuit designed in this study mainly consists of one extension unit and one flexion unit (Fig. 1(b) and (f)). Each unit is composed of a waist belt, two soft belts and two compact actuators with a control box (Fig. 1(d)). The actuators were mounted on the waist belt. The soft belt extended from the actuator was connected to the knee strap by the release buckle. The pulling force was generated between the waist belt and the knee strap when the soft belt was rolled up by a motor. The assistive forces were measured by load cells (FUTEK#FSH04099) attached between the knee straps and the ends of the soft belts (Fig. 1(g)). The thigh motion was measured by two inertial measurement units (IMU, MPU#9250), with each on one thigh (Fig.1(c)). The flexion and extension units were fixed on the front and back sides of the torso, respectively, providing the hip flexion and extension assistance. The gross weight of the system including the two assistance units was 4.7 kg.

A. Actuator Design

For each assistance unit, two compact actuators with symmetrical mechanical structures were designed (Fig. 1(b) and (f)). Figure 1(a) and (e) show the extension actuator and the flexion actuator, respectively. During walking, the stance leg undergoes a slow motion and supports the body weight as well as load carried, whereas the swing leg undergoes a relative fast motion but does not support loads, except for its own weight. Therefore, the flexion actuator must have a high responsiveness to provide a large pulling velocity, whereas it is crucial for the extension actuator to be able to provide a large torque. The actuators were configured as follows: a motor (flexion unit: Maxon EC 4-pole 22, 120 W, part #311537; extension unit: Maxon EC 4-pole 30, 200 W, part #305014) with a no load speed (flexion unit: 17800 rpm, extension unit: 16700 rpm) was connected to a gearbox with a reduction ratio (flexion unit: 14:1, extension unit: 33:1), and it drove a pair of upper and lower gears with a reduction ratio (flexion unit: 1:1, extension unit: 1:2.3). A reel with a radius of 1.3 cm connected to the lower gear was used to roll up the stiff belt. The actuators with configuration above not only provide the required torque while walking, but can easily follow the leg movements with a maximum pulling velocity of 1.73 m/s for the flexion unit, and 1.58 m/s for the extension unit.

The actuator was controlled by motor driver modules (flexion unit: ESCON 50/5, part # 438725; extension unit: ESCON Module 50/8, part # 532872). The modules in the control box were plugged into a custom circuit board (DSP, TMS320F28335) (Fig. 1(d)). The board was designed in two pieces, with one on the front chest and one on the back. Each board could process signals from two load cells and two IMUs, and they shared IMU signals to achieve coordination of hip flexion and extension assistance. Their powers were supplied by an external direct current power supply with 36 V.

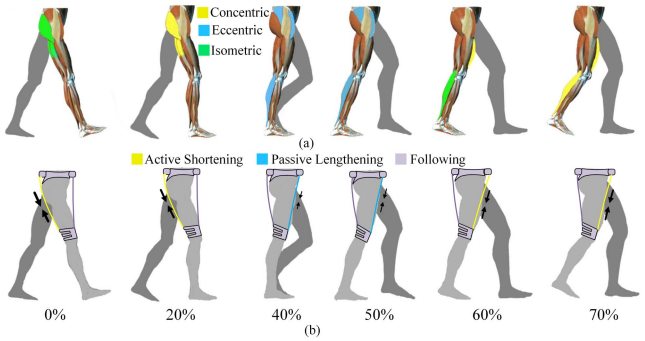

Fig. 2. (a) Sequence of muscle activation. The active muscles are highlighted with the colors, indicating if the muscles are shortening (concentric contraction), holding a fixed length (isometric contraction), or lengthening (eccentric contraction). (b) Diagrams of the exosuit. The color indicates if the belt is passive lengthening due to being stretched by the body's motion during high pretension, active shortening due to the belt retracting during positive power assistance, or following joint motion during low pretension. The size of the arrows indicates the force magnitude on the soft belt.

B. Biologically-Inspired Assistance

1) Analysis of Human Walking: It is necessary to understand the biomechanics of human walking for determining assistive force. Positive biological joint power occurs in muscle concentric (shortening) contractions in which the joint moment and joint motion are in the same direction [30], as in the hip extension positive power (HEPP) and hip flexion positive power (HFPP) phases (Fig. 3(a)). In the HEPP phase, hip extensor muscles shift from isometric to concentric activation, guiding the hip extension to lift the COM from its lowest point to the highest [24] (Fig. 2(a)). In the HFPP phase, rectus femoris and other hip flexor muscles contract concentrically to pull the leg swing forward [24] (Fig. 2(a)). In the two phases, a large increase in muscle forces of hip flexors and extensors was observed (Fig. 4(a)), estimated using AnyBody (vers.6.0, AnyBody Technology, Denmark), with similar result to those of Trinler *et al.* [31]. The increased muscle forces lead to a large consumption in metabolic energy to perform positive biological joint work. The belt-type soft exosuit creates the assistive force by active shortening the belt length, thus it easily imitates and replaces the work of these muscles in concentric contraction (Fig. 2(b)).

The muscles also consume metabolic energy to produce negative biological joint power that occurs in muscle eccentric (lengthening) contractions, in which the joint moment and motion are in opposite directions [30]. As in hip negative power (HNP) phase (Fig. 3(a)), hip flexor muscles, in particular the iliopsoas, controls the amount of hip extension through eccentric contraction (Fig. 2(a)) [24], which can be seen from the earlier increase in hip flexor forces (Fig. 4(a)). Additionally, the hip flexors and ligaments holding the femur to the pelvis also absorb some potential energy from the falling COM, and the energy is released to provide a positive power burst in the push-off period from 54% to 60% of gait cycle (GC) (Fig. 2(a)) [24]. Therefore, providing flexion directional force at the HNP phase is necessary for two main reasons: 1) imitating the eccentric contraction of the hip flexor muscles

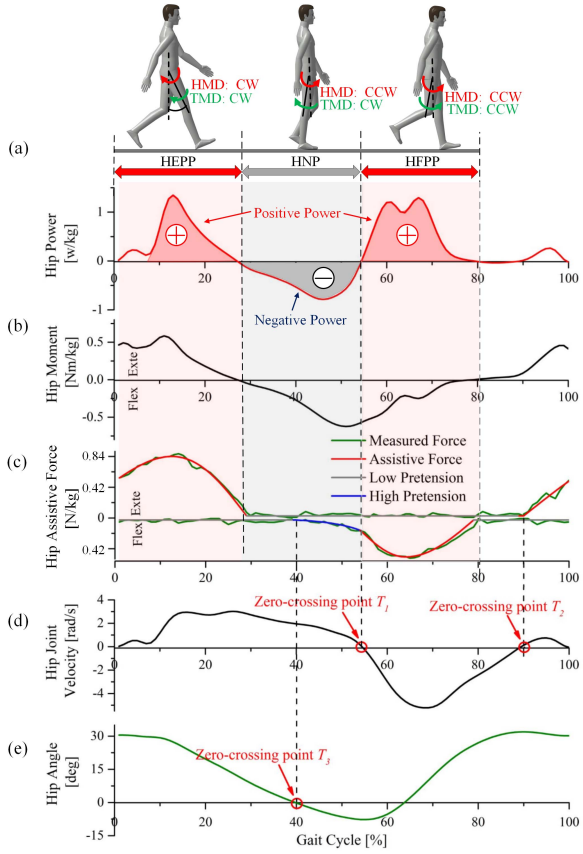

Fig. 3. Control approach. Typical kinematic and kinetic patterns of hip joint during a normal gait cycle: (a) joint power, (b) joint moment, (d) joint angular velocity and (e) joint angle. (c) assistive force and measured force under HFE assistance. Abbreviations: HEPP = hip extension positive power, HNP = hip negative power, HFPP = hip flexion positive power, HMD = hip moment direction, TMD = thigh movement direction, CW = clockwise, CCW = counterclockwise.

to control the amplitude of hip extension by passive lengthening of the belt (Fig. 2(b)); 2) providing the high pretension to actively absorb the elastic energy of the human-exosuit system in preparation for the later assistive positive power burst in push-off period.

2) Gait Segmentation Based on Zero-Crossing Detection: Gait was segmented by zero-crossing point detections of hip motion (Fig. 3(d) and (e)). T_1 and T_2 were two zero-crossing points of hip angular velocity, which were distinguished because they crossed the zero point from the positive and negative directions, respectively. T_3 was a zero-crossing point of hip angle. Time scale T_g of gait cycle was estimated by the time interval between two adjacent points T_2. High pretension at HNP phase was triggered at point T_3. Assistive forces at HEPP and HFPP phases were activated at the points T_2 and T_1. Time span of force profiles was defined as a certain percentage of T_g. This will be described in detail in following section.

3) Force Generation: The force of the exosuit could be classified into three, i.e. low pretension, high pretension and assistive force (Fig. 3(c)). The low pretension was constant so as to let the belts follow wearer's motion and maintaining an initial tension to prevent the soft belt taking off from

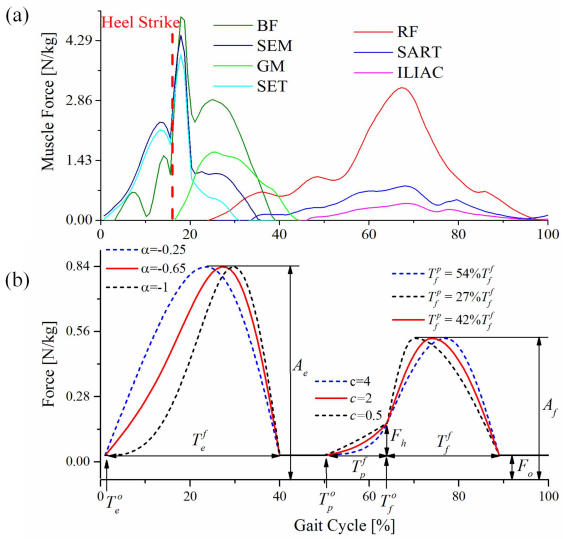

Fig. 4. Force profile. The gait cycle in the figure was segmented by the zero-crossing point T_2. (a) Muscle force. Hip extensor muscles: gluteus maximus (GM), biceps femoris (BF), semimembranous (SEM), and semitendinosus (SET). Hip flexor muscles: rectus femoris (RF), sartorius (SART), and iliacus (ILIAC). (b) Profile of HE is from 0% to 40%GC; Profile of HF is from 50% to 90%GC, in which includes the high pretension that ranges from 50% to 64%GC; Profile of HFE is from 0%−40%GC and 50%−90%GC.

the reel of actuator. The high pretension and assistive force were defined by functions, described in following section in detail.

a) High pretension at the HNP phase: Human-exosuit system is nonlinear and its stiffness is low. This results in a high hysteresis because the exosuit energy goes initially to stretching the spring instead of causing joint movement. Push-off period is short, during which lengthened muscles and ligaments provides a positive power burst to initiate swing. For a low stiffnesses system, assisting positive power burst is difficult in short time. Therefore, before the push-off, high pretension was applied to increase effective human-exosuit stiffness. Inspired by the human-exosuit stiffness test [32], the high pretension was defined as follows:

$$F_{pre}(t) = F_h \cdot \frac{\exp\left(c \cdot \frac{t-T_p^o}{T_p^f - T_p^o}\right) - 1}{\exp(c) - 1} + F_o, T_p^o \le t \le T_p^f, \tag{1}$$

where, F_o is a low pretension of 2 N; F_h is the amplitude of high pretension; c is a coefficient for adjusting the ascending slope of pretension. It was set to equal to 2 (Fig. 4(b), 50%−64GC) and the F_h was limited to 30% of the flexion force amplitude A_f, with a reference to the human-exosuit stiffness for maximizing comfort to wearer. T_p^o and T_p^f are start and offset timings. T_p^o was determined by zero-crossing point T_3. T_p^f was equal to the time interval between adjacent points T_1 and T_3.

b) Assistive force at the HFPP and HEPP phases: Two functions, proposed in our previous works [23], [28], were used to define the force profiles of hip extension and flexion assistance. Force profile at HFPP phase was defined as:

$$F_{flex}(t) = \begin{cases} \left(A_f - F_{pre}\left(T_p^f\right)\right) \sin\left(\frac{\pi(t - T_f^o)}{2(T_f^p - T_f^o)}\right) \\ \qquad + F_{pre}\left(T_p^f\right), \quad T_f^o \le t \le T_f^p \\ \left(A_f - F_o\right) \cos\left(\frac{\pi(t - T_e^p)}{2(T_f^f - T_f^p)}\right) + F_o, \\ \qquad T_f^p \le t \le T_f^f \end{cases} \tag{2}$$

where the force gradually increases from the high pretension maximum value F_{pre} (T_p^f); A_f represents the flexion force magnitude, T_f^o, T_f^p, and T_f^f denote start, peak, and offset timings, respectively. T_f^o was determined by the zero-crossing point T_1; T_f^p was set as 42% T_f^f for matching the peak timing of the HFPP phase (Fig. 4(b), 64%−90 GC). T_f^f was set as a 26% T_g that is an average percentage occupied by the HFPP phase. Force profile at HEPP phase was defined as:

$$F_{exte}(t) = (A_e - F_o) \sin\left\{\pi \frac{t - T_e^o}{T_e^f - T_e^o} + \alpha \sin\left(\pi \frac{t - T_e^o}{T_e^f - T_e^o}\right)\right\} + F_o, \quad T_e^o \le t \le T_e^f \tag{3}$$

where A_e represents extension force magnitude. α, T_e^o, and T_e^f denote waveform parameter, start and offset timings, respectively. T_e^o was determined by the zero-crossing point T_2. The peak timing was set to be 67% T_e^f (equivalent to $\alpha = -0.65$) for meeting the peak timing of the HEPP phase (Fig. 4(b), 0%−40GC). T_e^f was equal to 40% T_g as an average percentage occupied by the HEPP phase.

As shown in the Fig.4, the configured force profiles for hip flexion and extension assistance approximates that of the muscle forces of hip flexors and extensors, respectively. Considering the assistive performance and power limit of the system, the exosuit was designed to provide a 27% reduction in hip flexion/extension positive peak power at 1.39m/s walking speed, and the corresponding normalized average force amplitude was calculated as 0.83 N/kg for extension and 0.53 N/kg for flexion (Fig. 4(b)). The absolute force amplitude for each subject was assigned according to their body weight (Table I).

C. Control Scheme

To provide effective assistance and accurately transmit force to the wearer, closed-loop control of the assistive force was applied to track the desired force profiles in real time (Fig. 5). The force error was calculated by subtracting the desired force from the measured force obtained from the load cells. It was compensated in real time by a robust PID controller. The shape and timing span of the desired force profile were calculated by a certain percentage of T_g from the previous one GC, and then the profiles were triggered in real time at the three zero-crossing points (T_1, T_2, and T_3) from the current gait information of the IMUs. The low pretension on the soft belt was kept if the three zero-crossing points were not detected.

TABLE I
PARAMETERS OF EIGHT SUBJECTS

Subject Number	1	2	3	4	5	6	7	8	Mean±SD
Age(years)	26	24	24	24	24	27	26	32	25.8±2.7
Height (cm)	183	175	170	172	173	175	183	174	175.6±4.8
Weight (kg)	67	75	56	89	68	74	80	73	72.7±9.7
Force amplitude (N) (Extension / Flexion)	56/35	62/40	46/30	74/47	56/36	61/39	66/42	61/39	60.8±8.6 / 39±5.2

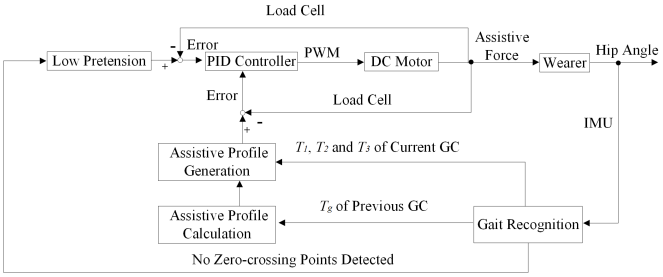

Fig. 5. Block diagram of the force control scheme.

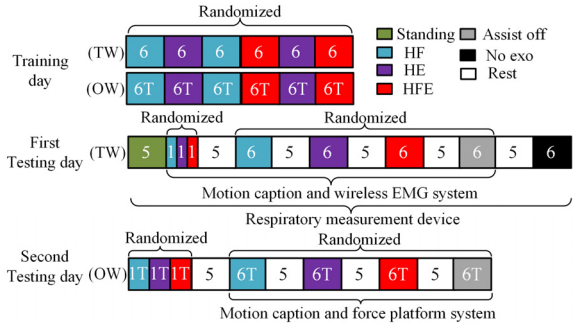

Fig. 6. Testing protocol during training and testing days. Numbers in each block represent the duration of each condition, in which the 1T and 6T indicate 1 time and 6 times overground walks of one-way straight path. TW = Treadmill walking; OW = Overground walking.

III. EXPERIMENTAL EVALUATION

We conducted walking tests on eight healthy subjects under three hip assistance modes, in which the metabolic powers, power efficiencies, muscle activity, kinematics, and kinetics were analyzed. All subjects received explanations about the nature and possible consequences of the tests and provided written informed consent before their participation. The study was approved by the Biomedical Ethics Committee of Hebei University of Technology in Tianjin, China.

A. Subjects

We recruited eight male subjects (n=8) who participated in the experiment. All of them were young and healthy adults (no musculoskeletal injuries or diseases). Table I lists their details.

B. Protocol

The experimental protocol was separated into one training day and two testing days (Fig. 6). On the training day, each subject worn the exosuit walked on a treadmill (SportArt Fitness, Wisconsin, USA) at a constant speed of 1.39 m/s to let them become familiar with the exosuit, during which they conducted 6 randomized 6-minute walking bouts, experiencing each of the 3 assistance modes (HF, HE, and HFE) twice. Brief rests were allowed between the conditions according to their own requests. The subjects then performed overground walking with a straight path. They were trained to expect a constant speed of 1.39m/s when they passed the floor with an embedded biomechanics force platform (four 90 × 60cm 9287C plates, Kistler, Winterthur, Switzerland, 1000Hz) at the end of a 10-meter one-way straight path (Fig. 7(d)). The constant walking speed was controlled by limiting their stride length and stride frequency using ground markers and metronome, respectively. They walked for 6 randomized bouts, experiencing each assistance mode twice. Adequate training on an average of 6 times consecutive straight path walks was given in each bout. Subjects rested between the bouts according to their own requests.

On the first testing day, each subject who wore the exosuit was firstly asked to attend a 5-minute standing test to collect standing metabolic data. Then they were asked to attend the walking tests on a treadmill. After a 3-minute treadmill walking warm-up (1 minute for each assistance mode), the subjects took a rest of 5 minutes. After the above preparation, they were instructed to walk on the treadmill with a constant speed of 1.39 m/s (Fig. 7(a)), and underwent four 6-minute walking bouts: 3 with the conditions (HF, HE, and HFE) and 1 with assist off condition with the device. The order in which these conditions were presented was randomized for each subject to avoid fatigue or learning effects. Finally, each subject removing the exosuit completed a 6-minute walking bout on the treadmill. An adequate rest on an average of 5 minutes was given between walking bouts for physical recovery.

On the second testing day, each subject who wore the exosuit was asked to perform 3 times warm-up overground walks of straight path (1 time for each assistance mode). After a rest of 5 minutes, a rectilinear overground walking test with embedded force platform in the floor (Fig. 7(c)) was performed, during which each subject underwent four walking bouts: 3 at assist on conditions and 1 at assist off condition, in which six times consecutive straight path walks was performed for each walking bout. The order of the four conditions was randomized, and a 5-minute rest was interleaved between the walking bouts.

During treadmill walking, metabolic data were collected by wearing a portable respiratory measurement device

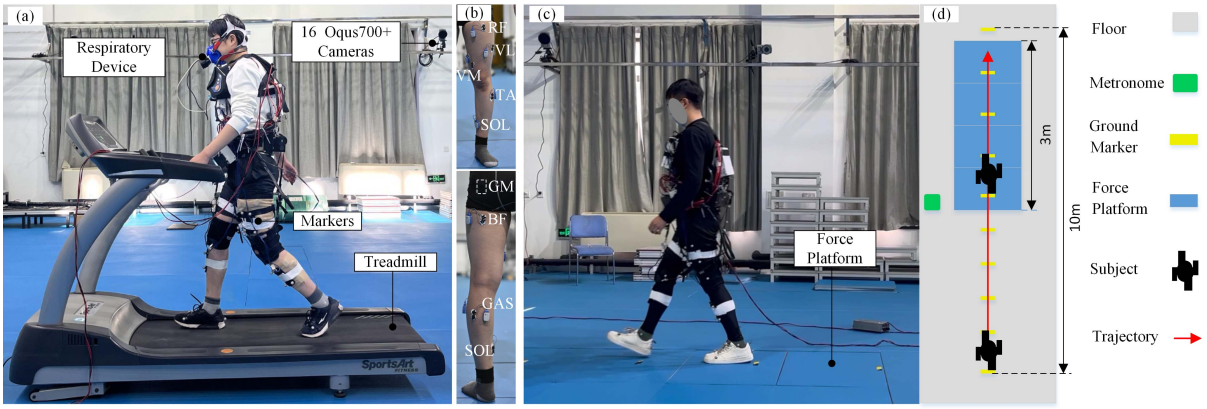

Fig. 7. Experimental scenario. (a) Treadmill walking. (b) EMG sensor placement. (c) Overground walking on the floor embedded with biomechanics force platform. (d) Gait course of overground walking. The metabolic powers, power efficiency, kinematics and muscle activity were assessed from treadmill walking. The kinetics were calculated from the walking on force platform.

(MetaMax3B-R2, Cortex, Leipzig, Germany). Surface electromyography (EMG) signals were measured by means of a wireless system (Noraxon, Ultium Emg, USA; 2000 Hz). Electrodes were placed on body following SENIAM guidelines [33] (Fig. 7(b)). During overground walking, GRF data were obtained from the force platform system embedded in the floor. Kinematic data were collected through a 16-camera optical motion capture system (Qualisys, Göteborg, Sweden; 300 Hz). Totally 44 reflective markers were used in the tests, with 36 placed on body and 8 on the soft belts of the exosuit. Additionally, the wearing state and mass of the exosuit was constant across the HF, HE, HFE, and assist off conditions.

C. Data Processing

1) Treadmill Walking:

a) Metabolic power: Oxygen consumption (V_{O2} [L/min]) and respiratory quotient (C_{RQ}) were averaged across the last two minutes of standing and each treadmill walking conditions, and then used to calculate the standing and walking metabolic powers using a well-known Zuntz regression equation [34], [35], [36]. Net metabolic power (P_{net}) was obtained by subtracting the standing metabolic power from the walking metabolic power, and then was normalized by the body mass of each subject.

b) Assistive power and efficiency: The assistive powers of the exosuit were calculated as follows:

$$\begin{aligned} P_{flex} &= P_{pre}^{(-)} + P_{flex}^{(+)} \\ &= -\frac{\sum_{i=1}^{n_1} l_{flex}(i) \cdot F_{pre}(i) \cdot w_{hip}(i)}{n_1} \\ &\quad + \frac{\sum_{i=1}^{n_2} l_{flex}(i) \cdot F_{flex}(i) \cdot w_{hip}(i)}{n_2}, \end{aligned} \tag{4}$$

$$P_{exte} = \frac{\sum_{i=1}^{n_3} l_{exte}(i) \cdot F_{exte}(i) \cdot w_{hip}(i)}{n_3} \tag{5}$$

where P_{flex} and P_{exte} represent flexion and extension directional assistive powers, respectively, calculated by discrete sampled data points; $P_{pre}^{(-)}$ and $P_{flex}^{(+)}$ represent negative and positive flexion assistive power, respectively; n_1, n_2, and n_3 are the number of sampled data points; $l_{flex}(i)$ and $l_{exte}(i)$ indicate the flexion and extension moment arms; $F_{pre}(i)$, $F_{flex}(i)$, and $F_{exte}(i)$ represent the high pretension, flexion and extension assistive forces, respectively; $w_{hip}(i)$ is the hip angular velocity. The total assistive power P_{exo} of the exosuit was calculated as follows:

$$P_{exo} = P_{flex} + P_{exte} \tag{6}$$

The P_{exo} was normalized by subject's body mass. The metabolic energy expenditure related to external work represents only a portion of the net metabolic energy, and the remainder appears as heat. The walking metabolic power P_{walk} accounts for a proportion ($\eta_{walk} = 10\sim30\%$) of the net metabolic power P_{net} [37], and it is defined as follows:

$$P_{walk} = \eta_{walk} \cdot P_{net}. \tag{7}$$

The reduction P_{redw} in walking metabolic power was obtained by subtracting the P_{walk} in the assistance turned on (assist on) condition from that in the assistance turned off (assist off), as follows:

$$P_{redw} = P_{walk(assist-off)} - P_{walk(assist-on)}. \tag{8}$$

The power efficiency η_{exo} of the exosuit was expressed by dividing P_{redw} by P_{exo} as follows:

$$\eta_{exo} = P_{redw}/P_{exo}. \tag{9}$$

For HFE assistance, it is hypothesized that the two directional effects of assistance on the metabolic reduction are independent of each other and operate in parallel. The parallel efficiency η_{exo}^{p} was calculated as a linear superposition of η_{exo}^{f} and η_{exo}^{e}, as follows [38]:

$$\eta_{exo}^{p} = (\eta_{exo}^{f} \cdot P_{flex} + \eta_{exo}^{e} \cdot P_{exte})/P_{exo}, \tag{10}$$

where, η_{exo}^{f} and η_{exo}^{p} represent the power efficiencies of HF and HE assistance, respectively; P_{flex}, P_{exte}, and P_{exo} were obtained from HFE assistance.

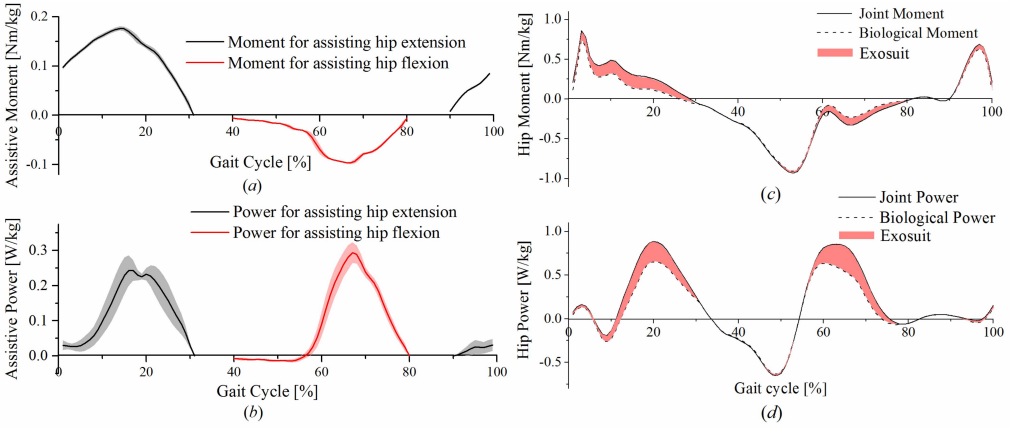

Fig. 8. Measured moment and power from the overground walking in the floor embedded with force platform under HFE assistance. Data are group means (n = 8). (a) and (b) Assistive moment and power. The standard deviations are shown with light shading of same color. (c) and (d) Hip moment and power. The moment and power applied by the exosuit are represented using the shaded regions.

c) Joint Kinematics: Joint kinematic data from treadmill walking were analyzed using Qualisys Track Manager (Qualisys, Göteborg, Sweden) and Visual 3D (C-motion, Germantown, MD, USA). Joint angles were calculated in the sagittal plane by a model analysis with 36-marker protocol [39]. Heel strikes defined gait cycle were determined approximatively using heel-marker data. Ten gait cycles were used to acquire mean data for each participant.

d) Muscle activity: Muscles investigated were: rectus femoris (RF), vastus medialis (VM), vastus lateralis (VL), gluteus maximus (GM), biceps femoris (BF), soleus (SOL), Gastrocnemius Lateralis (GAS), and tibialis anterior (TA) (Fig. 7(b)). These muscles were chosen for highlighting potential differences between the different assistance conditions on lower limb joints. Raw EMG signals were band-pass filtered (4th order Butterworth, cut-off 20–450 Hz) to remove electrical noise and biological artifacts, then signals were rectified and low-pass filtered (4th order Butterworth, cut-off 6 Hz) to obtain a linear envelope, and lastly normalized by average amplitude of the EMG recorded during the assist off condition. Root mean square (RMS) was calculated from each normalized curve from the last minute of walking data. The change of EMG RMS was calculated by subtracting the RMS value in assist off condition from that in assist on.

2) Overground Walking:

a) Joint kinetics: Joint kinetic data from overground walking were analyzed. Joint moments and joint powers were calculated in the sagittal plane by an inverse dynamic analysis in combination with 36-marker kinematics and GRFs using the visual 3D. Heel strikes were identified from GRFs and marker data. All kinetic data including moment, power, work, GRF, and acceleration of the COM were averaged from ten gait cycles with stable gait and then normalized by the body mass of each subject.

b) Biological power and work: Additional eight markers were placed on soft belts, two markers on each belt. Moment arms were defined as the perpendicular distance in the sagittal plane between the markers on the soft belt and hip joint center. The assistive moment was calculated as the product of assistive force recorded by the load cells and the moment arm (Fig. 8(a)), and then multiplied by the hip joint velocity to obtain assistive power (Fig. 8(b)). Biological hip moment was calculated by subtracting the assistive moment from the hip moment in the assist on condition (Fig. 8(c)). Similarly, the biological hip power was also obtained as following the method as above (Fig. 8(d)). Positive and negative biological joint work were calculated by integrating over time the corresponding positive and negative biological joint powers.

c) Acceleration of the COM: Vertical acceleration of the COM was calculated using the resultant vertical GRF (minus body weight) of both legs divided by the body mass. Horizontal acceleration of the COM was equal to the resultant horizontal GRF divided by the body mass [40].

D. Statistical Analysis

Means and standard deviations for each test condition were calculated. One-way repeated measures analyses of variance (ANOVA) with three conditions (HFE, assist off, and no exo) were used to verify the effect of the device on metabolic reduction. Additionally, the one-way repeated ANOVA including four conditions (HF, HE, HFE, and assist off) were also conducted to verify the effect of assistance on net metabolic power, power efficiency, peak GRF, peak acceleration of the COM, peak joint angles, peak moments, peak powers (hip, knee, and ankle) as well as positive and negative biological joint work (total and single joint). Pairwise comparisons with Bonferroni post hoc tests were conducted to identify differences between conditions when a statistically significant main effect was identified by the ANOVA. Paired t tests were performed to assess the difference in EMG RMS between assist on and assist off condition for each assistance mode. It was also conducted to assess the difference in assistive power, metabolic reduction and reduced total biological joint work between HFE and sum of effects of HF and HE. $p<0.05$ represents a significant difference.

IV. Results

A. Metabolic Power

Compared with assist off condition, the average net metabolic power was reduced significantly in each assistance

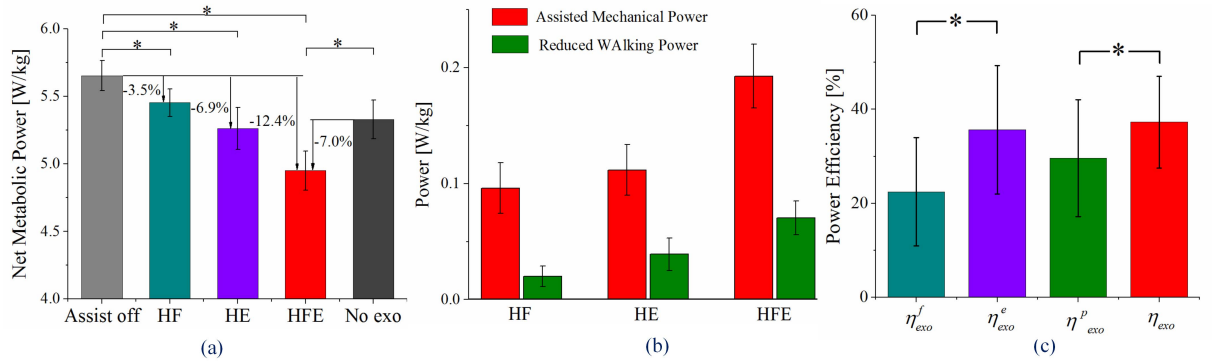

Fig. 9. Net metabolic power and efficiency. (a) Net Metabolic power. (b) Assisted mechanical power was calculated using the Eq. (4) to (6), and reduced walking power P_{redw} was required by the Eq. (7) and (8) according the lowest walking efficiency η_{walk} =10%. (c) Power efficiency. η^{f}_{exo}, η^{e}_{exo} , and η_{exo} indicate the power efficiency of HF, HE, and HFE assistance, respectively, calculated using Eq. (9). η^{p}_{exo} indicates parallel power efficiency, calculated by Eq. (10). Data are group means $\pm$ SD (n = 8). * Significant difference at p<0.05.

mode (Fig. 9 (a)) (assist on vs. off, n = 8, p < 0.03). The average relative reduction was 3.5 $\pm$ 1.5 % (HF), 6.9 $\pm$ 2.4 % (HE), and 12.4 $\pm$ 2.5 % (HFE). The HFE assistance provided a larger reduction than the sum of HF and HE (two-sided paired t tests, n = 8, p = 0.006), and the HE assistance also reduced a more metabolic power than HF (n = 8, p = 0.04). Additionally, compared with not wearing the exosuit, HFE assistance reduced metabolic power by 7% $\pm$ 3.8% (HFE vs. no exo, n = 8, p = 0.001).

B. Supplied and Reduced Power

The average assistive power of eight subjects was 0.09 $\pm$ 0.02 W/kg (HF), 0.11 $\pm$ 0.02 W/kg (HE), and 0.19 $\pm$ 0.03 W/kg (HFE) (Fig. 9(b)), with corresponding the reduced average walking power of 0.02 $\pm$ 0.01 W/kg, 0.04 $\pm$ 0.01 W/kg, and 0.07 $\pm$ 0.01 W/kg relative to the assist off condition. The HFE assistance provided a somewhat lower assistive power than that of the sum of HF and HE (two-sided paired t tests, n = 8, p = 0.054), whereas the reduced walking power was higher than the sum of HF and HE (two-sided paired t tests, n = 8, p = 0.006).

C. Power Efficiency

Power efficiencies of three assistance modes were assessed relative to assist off condition (Fig. 9(c)). The average power efficiency of eight subjects was 22.4 $\pm$ 11.5% (HF), 35.6 $\pm$ 13.6% (HE), and 37.3 $\pm$ 9.7% (HFE) (Fig. 8 (c)). The HE assistance provided a higher power efficiency than the HF (n = 8, p = 0.001). A parallel power efficiency of 29.6 $\pm$ 12.4% was calculated as a linear superposition of the HF and HE. The average power efficiency of HFE assistance was higher than the parallel efficiency (n = 8, p = 0.002).

D. Kinematics

Under the HF, a greater peak hip flexion angle and a smaller peak hip extension angle were found (assist on vs. off, n=8, p < 0.005) (Fig. 10(a)). For the HE, a greater peak hip extension angle and a smaller peak hip flexion angle were observed (assist on vs. off, n = 8, p < 0.004). Under the HFE, a larger hip flexion peak angle and a larger hip extension peak angle were observed (assist on vs. off, n = 8, p < 0.004). Peak knee flexion angle (Fig. 10(a), 67%−100% GC) under HF and peak knee extension angle (0%−67% GC) under HE were increased (assist on vs. off, n = 8, p < 0.004). Under the HFE, a larger knee flexion peak angle and a larger knee extension peak angle were observed (assist on vs. off, n = 8, p < 0.001). Similarly, the peak ankle dorsiflexion and plantarflexion angles were increased under the HFE (assist on vs. off, n = 8, p < 0.005).

E. Kinetics

1) Joint Moment: Biological hip moments in corresponding assistance phases were reduced (Fig. 10(b), 10%−30% GC and 60%-80% GC, assist on vs. off, n = 8, p < 0.002). A smaller peak knee flexion moment in the stance phase and a larger peak ankle dorsiflexion moment were found under the HE and the HFE (assist on vs. off, n = 8, p < 0.001). The increase in peak ankle moment was larger for the HFE than that for the HE (HFE vs. HE, n = 8, p = 0.005). No significant changes were seen at the knee and ankle moments under the HF.

2) Joint Power: Positive biological hip powers in corresponding assistance phases were reduced (Fig. 10 (c), 10%−30% GC and 60%-80% GC, assist on vs. off, n = 8, p < 0.004). For the HE and HFE, the positive and negative peak knee powers were reduced (assist on vs. off, n = 8, p < 0.001), and the negative peak ankle dorsiflexion power (30%-50% GC) was increased (assist on vs. off, n = 8, p < 0.011). The HFE assistance caused a trend toward a larger increase in the negative peak ankle dorsiflexion power than that under the HE (HFE vs. HE, n = 8, p = 0.058). Additionally, no significant change was found for the knee and ankle power under the HF.

3) Joint Work: Under the HE assistance, the total biological joint positive work (sum of hip, knee, and ankle) had a reduction (assist on vs. off, n = 8, p = 0.046) (Fig. 11), in which the significant reductions were occurred in hip and knee joints (assist on vs. off, n = 8, p < 0.047). The total positive work was not significantly changed under the HF.

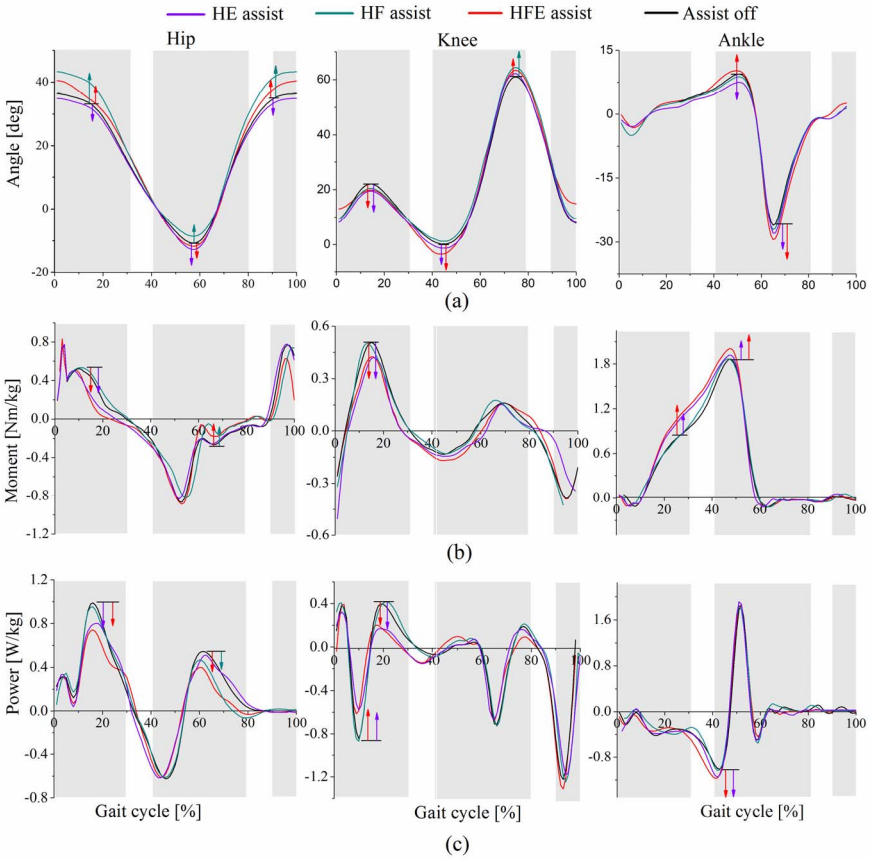

Fig. 10. Joint kinematics and kinetics. (a) Positive and negative angles represent flexion and extension. (b) Positive and negative moments represent net extension and flexion joint moments. (c) Positive and negative powers represent instantaneous energy generation and absorption [41]. Data are group means (n = 8). Gray shaded regions indicate hip assistance periods at a gait cycle. The arrow indicates significant difference at $p<0.05$, and a longer arrow indicates a higher significance level. Its direction points to the changed profile in the assist on condition relative to that in the assist off.

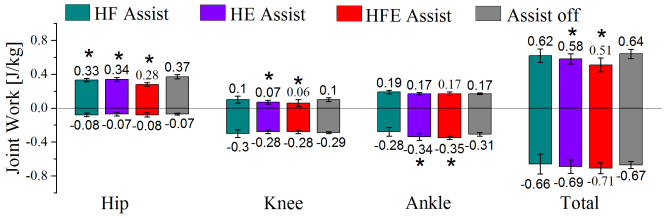

Fig. 11. Positive and negative biological joint works. Positive work represents energy generation, and negative work represents energy absorption [41]. Data are group means ± SD (n = 8). * Significant difference level (assist on vs. off, $p < 0.047$).

For the HFE, the reduction in total positive work was larger than that for the sum of the HF and the HE (0.13 J/kg vs. 0.08 J/kg, two-sided paired t tests, n = 8, p = 0.04). No significant change in total negative work for the three assistances was found.

4) Ground Reaction Force: Under the HE and the HFE assistance, the peak vertical and horizontal GRFs were increased (Fig. 12, 0%−30% GC, assist on vs. off, n = 8, $p < 0.003$), which means that the resultant GRF was increased. For the HF assistance, the peak vertical and horizontal GRFs were not changed significantly.

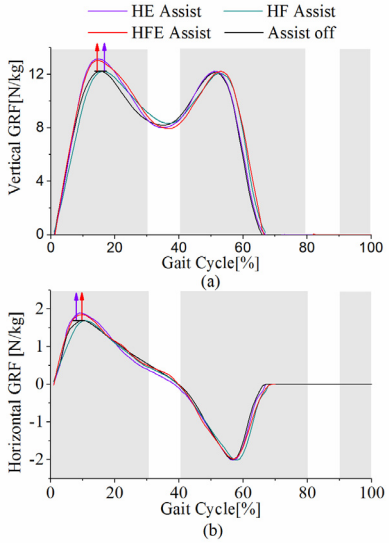

Fig. 12. GRF. (a) and (b) show vertical and horizontal GRFs. Data are group means (n = 8). The gray shaded regions indicate assistance periods. The effect of the arrows is depicted in the caption of Fig. 9.

5) Acceleration of the COM: A larger peak vertical upward acceleration of the COM under the HE and a larger peak vertical downward acceleration under the HF were observed

TABLE II
COMPARISON OF TYPICAL EXOSKELETONS WITH HIP ASSISTANCE

Study	Joint Assisted	Device type	Peak force	Comparison performed	Metabolic reduction
Ding *et al.* [20]	Hip extension	Powered, off-board tethered actuation	100N	Assist on vs. off	4.6 %
Kim *et al.* [22]	Hip extension	Powered, cable actuator	300N	Assist on vs. off or no exo	15.4 % or 9.3 %
Jin *et al.* [18]	Hip flexion	Powered, belt-type actuator	30N	Assist on vs. off	5.9 %
Panizzolo *et al.* [44]	Hip flexion	Unpowered, elastic element	about 53N	Assist on vs. no exo	3.3 %
Zhou *et al.* [45]	Hip flexion	Unpowered, elastic element	/	Assist on vs. no exo	7.2 %
Panizzolo *et al.* [42]	Hip extension, hip flexion and ankle plantarflexion	Powered, cable actuator	68N, 204N, 272N	Assist on vs. off or no exo	14.2 % or 7.3 %
Kang *et al.* [26]	Hip flexion and extension	Powered, ball screw actuator	/	Assist on vs. off	6%
Chen *et al.* [28]	Hip flexion and extension	Powered, belt & cable actuator	130N, 50N	Assist on vs. off	8.5 %
In this study	Hip extension	Powered, belt-type actuator	61N	Assist on vs. off	6.9 %
	Hip flexion		39N	Assist on vs. off	3.5 %
	Hip flexion and extension		39N, 61N	Assist on vs. off or no exo	12.4 % or 7 %

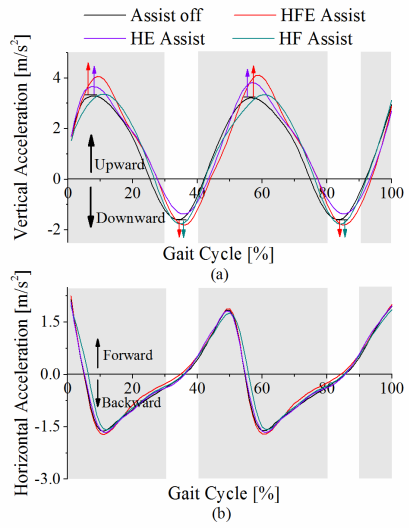

Fig. 13. Acceleration of the COM. (a) and (b) show vertical and horizontal accelerations. Data are group means (n = 8). The gray shaded regions indicate the assistance periods. Black arrows indicate the direction of acceleration, whereas the effect of the colored arrows is depicted in the caption of Fig. 9.

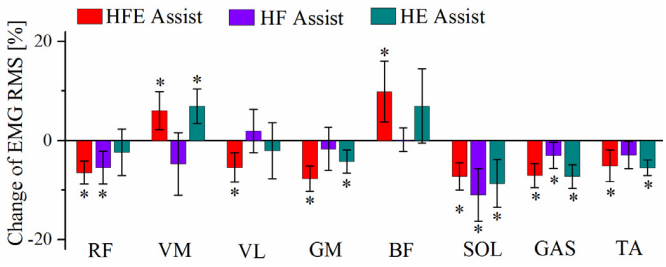

Fig. 14. Change in the EMG RMS during HFE, HF, and HE assistances compared to assist off. Data are group means ± SD (n = 6). Negative value represents reduction. RF = Rectus Femoris, VM = Vastus Medialis, VL = Vastus Lateralis, GM = Gluteus Maximus, BF = Biceps Femoris, SOL = Soleus, GAS = Gastrocnemius Lateralis, TA = Tibialis Anterior. * Significant difference between assist on and assist off condition at $p < 0.048$.

(assist on vs. off, n = 8, $p < 0.001$) (Fig. 13(a)). For the HFE assistance, larger peak vertical upward and downward accelerations of the COM were found (assist on vs. off, n = 8, $p < 0.027$). Horizontal acceleration of the COM was not changed significantly (Fig. 13(b)).

F. EMG Analysis

Under the HFE condition, a significant reduction in the EMG activity was observed in six subjects for the majority of the muscles, except for the VM and the BF (Fig. 14). The RF, VL, and GM of the thigh were reduced by 6.47 ± 2.28 %, 5.44 ± 2.95 %, and 7.68 ± 2.57 % (assist on vs. off, two-sided paired t tests, n = 6, $p < 0.007$), respectively. The reductions in the muscles of the shank were 7.2 ± 2.75 % (SOL), 7.06 ± 2.44 % (GAS), and 5.1 ± 3.18 % (TA) (assist on vs. off, two-sided paired t tests, n = 6, $p < 0.012$). The HE assistance reduced the EMG activities of the GM, SOL, GAS, and TA (assist on vs. off, two-sided paired t tests, n = 6, $p < 0.008$) to an almost same level as the HFE. For the HF assistance, a significant reduction was observed in the RF, SOL, and GAS (assist on vs. off, two-sided paired t tests, n = 6, $p < 0.047$), with a maximum reduction of 10.96 ± 5.3% for the SOL.

V. DISCUSSION

In this study, we developed a belt-type soft exosuit to provide bi-directional (hip flexion and extension) assistance for augmenting walking. Assistive strategy of the exosuit was presented considering the contraction mechanisms of hip flexor and extensor muscles. The HFE assistance was compared with the HF and HE by an evaluation on biomechanics and physiology for eight subjects. Significant advantage of the HFE assistance was observed in the results.

An extensive comparison of some typical exoskeletons with hip assistance is presented in Table II. In this study, the HE assistance reduced the metabolic power by 6.9 ± 2.4 %, corresponding the delivered mechanical power of 7.9 ± 0.87 W with an average peak force of 60.8 N, whereas in [20], a reduction of 4.6 ± 0.8 % was reported, with delivered mechanical power of 7.04 ± 0.7W and a peak force of 100 N using an off-board tethered actuation. Additionally,

in this study, a 61 N force amplitude produced an extension moment of 12.15 Nm, whereas in [42], a 68 N force produced that of only approximately 9.73 Nm by a cable actuator, which is attributed to a larger moment arm generated by the presented belt-type soft exosuit. These comparisons show the advantages of our device. A study in [22] reported a considerable metabolic reduction, with delivered mechanical power of 9.78 $\pm$ 3.05W under a peak force of 300N. It shows that a large force amplitude is necessary for hip extension to achieve greater metabolic reduction.

In this study, for the HF assistance, an average metabolic reduction was 3.5 $\pm$ 1.5% for 8 health subjects, whereas a similar study in [18] reported a reduction of 5.9% for 9 elderly subjects. Perhaps, the elderly groups are more sensitive to the hip flexion assistance due to them demand for improving gait. Additionally, some studies on unpowered exosuits [43], [44], [45], using elastic element to recycle part of the negative biological energy produced by hip extension and then releasing the stored energy during hip flexion, reported metabolic reductions of 3.3 $\pm$ 3.0% in [44] and 7.2 $\pm$ 1.2% in [45]. Similar study by Collins *et al.* [46] was also presented for ankle plantarflexion assistance. These provide an inspiration that, like adjusting passive spring stiffness, reasonable controlling the level of negative assistive work may be a key for effective hip flexion assistance.

In this study, the HFE assistance reduced metabolic power by 12.4 $\pm$ 2.5 % and 7% $\pm$ 3.8 % relative to assist off and no exo, respectively. This is greater than that of previous work by our lab in [28]. Similar level in metabolic reduction was reported in [42]. It involved ankle assistance and higher force amplitudes applied than this study. Further a study in Lee *et al.* [47] using a similar device to [42], reported a higher metabolic reduction of 14.8 % relative to no exo. Such results may be attributed to its higher force amplitude applied than in [42] and online parameter tuning algorithm, which is a direction of our efforts in future. Compared to a hip rigid exoskeleton in [26], metabolic advantage of our device may be due to the low constraint on natural joints at no-assisted phase of gait cycle, because of nature low stiffness of soft exosuits than the rigid.

Interestingly, in this study, the HFE assistance provided a larger metabolic reduction than the sum of HF and HE (Fig. 9(a)). However, it is worth noting that the exosuit seems sensitive to the body mass and height of the wearer. Initially HFE for the three subjects (No. 3, 5, and 7) did not show significant advantage over the sum of HF and HE on metabolic reduction, but after adjusting the sizing of the soft components of the exosuit for each subject and retesting them, then significance of HFE was found. This means that matching the exosuit to the body of the wearer is important for getting sufficient assistance. For a walking assistive device, higher power efficiency means reducing more walking power expenditure with less assistive power injection. The power efficiency of the HFE assistance was higher than the parallel efficiency of HF and HE (Fig. 9(c)), demonstrating that its effect on metabolic reduction cannot be considered as a simple linear superposition of its two directions. The effect of gait on altering metabolic power cannot be ignored [48], [49]. The HFE assistance may improve the gait, further contributing to a larger metabolic reduction.

In terms of kinematics, for the HE assistance, an increase of hip extension peak angle and a reduction of hip flexion peak angle were observed, which is consistent with the findings by Ding *et al.* [20]. For the HF assistance, the change of hip angle was reverse to that of the HE (Fig. 10(a)). These results suggest that the assistance augments the motion of the assistive direction, while weakening the motion opposite to the assistive direction. The HFE assistance can enable joint motion to achieve a balance in flexion and extension directions, thus maintaining a relatively natural gait. This may be conducive to contributing a lower metabolic power.

In terms of kinetics, the three hip assistance modes provided different reductions in hip biological joint moment and power (Fig. 10(b) and (c)). The knee and ankle were also indirectly affected. Under HE assistance, the peak knee flexion moment in the stance phase was reduced, which is consistent with the findings by Kim *et al.* [22], and the positive and negative peak knee powers were reduced. The contribution of reduced knee kinetics to metabolic reduction has been demonstrated [50]. With similar principle, Wu *et al.* [19] and Park *et al.* [51] developed a hip extension assisted soft exosuit, with a knee lever mechanism for amplified knee extension function used to uphill walking or stair climbing. The ankle dorsiflexion moment and negative ankle dorsiflexion power were increased, which may explain the decrease in peak knee power because the extension assistance weakens the knee joint effect as a shock absorber [52] while augmenting ankle kinetics, thus forcing the ankle to more powerfully propel the body upward and forward. These changes in kinetics were more significant under the HFE, which may be due to flexion directional assistance increasing the amplitude of the forward swing of the legs, thus leading to a greater reliance on the extension assistance for pulling back the standing leg in the next phase. Whether these changes in kinetics all are beneficial to metabolic reduction has not been verified. However, it was worth noting that these changes contributed to a reduction in the total biological joint positive work, which is conducive to the metabolic reduction. Furthermore, the reduction in total positive work under HFE was larger than the sum of HF and HE (Fig. 10), demonstrating that the synergistic effect of the HFE assistance is significant for reducing more biological work and more metabolic power.

The HE assistance increased the peak vertical and horizontal GRFs (Fig. 12), thus leading to an increase in the peak upward acceleration of the COM (Fig. 13(a)). The HF assistance applied a downward inertia force to the COM, increasing the peak downward acceleration of the COM. The HFE increased the peak upward and downward accelerations of the COM due to a superimposed effect of two directional assistances on the COM. These imply an increase in the translation force exerted at the COM provided by the assistance of the exosuit [53]. It effectively promotes the energy exchange of the COM between potential and kinetic energy, which is conducive to reducing the consumption in biological mechanical work for transferring the COM [54], [55] and reducing more metabolic power.

The EMG results in two of the eight subjects were not used, mainly due to inexperience in the initial test resulting in electrodes interfered by the textile of the exosuit and even slipping on the skin. Significant reductions in muscle activity were observed in remaining six subjects. For the HF assistance, significant EMG reductions in the RF, SOL, and GAS were seen (Fig. 14) because the assistance was applied at push-off and subsequent swing phases, during which these muscles have a major effect [24]. Under the HE assistance, an EMG reduction in hip extensor muscle (GM) was observed. Additionally, the muscle activities (SOL, GAS, and TA) of the shank also were reduced, which is almost consistent with the results in [22]. The weakened knee kinetics may lead to the reduced muscle activities of the shank. In contrast, increased ankle kinetics may be linked to the changes in the functional properties of the muscles, rather than simply being a reduction of muscle activation. For the HFE assistance, a reduction in the activity of more related muscles was found, including hip flexor muscle (RF: -6.47 %), hip extensor muscle (GM: -7.68 %), knee extensor muscle (VL: -5.44 %), and these muscles (SOL, GAS, and TA) of the shank (Fig. 13). These reductions may be attributed to the multi-muscle synergistic effect of HFE assistance for both legs. For individual subjects, these muscle activities showed a large reduction (GM: -9.72 %, RF: -8.25 %, VL: -7.9 %, assist on vs. off, two-sided paired t tests, $n = 3$, $p < 0.016$). A study on pneumatic soft exosuit for the HFE assistance by Thalman *et al.* [27] reported a larger EMG reduction (GM: -13.1 %; RF: -27.7 %, $n = 3$). This may be due to its higher force amplitude setting than this study.

Last, it is worth noting that we did not conduct comparison between the assist on and no exo condition for these data: the power efficiencies, kinematics, kinetics, and muscle activities; instead, the assist off condition was used as a baseline of the comparison between the assistance modes. This choice was taken to avoid increased variability due to repositioning the markers and electrodes after removing the exosuit.

VI. Conclusion and Future Work

We developed a belt-type soft exosuit and presented an assistive strategy of hip bi-directional (HFE: hip flexion and extension) assistance. The HFE assistance was compared with the two uni-directional assistances: hip flexion (HF) and hip extension (HE) by tests on eight subjects. An evaluation on biomechanics and physiology was performed for all subjects under the three assistance modes. It was demonstrated that the HFE assistance could achieve a greater metabolic reduction than the sum of HF and HE. HFE could also reduce more total biological joint work and the activity of more muscles. Furthermore, it could increase the upward and downward accelerations of the COM, thus raise the walking efficiency by promoting the energy exchange between potential and kinetic energy. Overall, the HFE assistance can not only reduce metabolic power, but also has a synergistic effect.

This work provides a reference for design and optimization of hip-assisted soft exosuits. In the future, we will optimize the force profile configurations for the HFE assistance under different walking conditions.

References

[1] A. D. Kuo, J. M. Donelan, and A. Ruina, "Energetic consequences of walking like an inverted pendulum: Step-to-step transitions," *Exerc. Sport Sci. Rev.*, vol. 33, no. 2, pp. 88–97, 2005.

[2] J. M. Donelan, R. Kram, and A. D. Kuo, "Mechanical work for step-to-step transitions is a major determinant of the metabolic cost of human walking," *J. Exp. Biol.*, vol. 205, no. 23, pp. 3717–3727, 2002.

[3] R. M. Aspden, K. E. Rudman, and J. R. Meakin, "A mechanism for balancing the human body on the hips," *J. Biomechanics*, vol. 39, no. 9, pp. 1757–1759, Jan. 2006.

[4] G. A. Cavagna, H. Thys, and A. Zamboni, "The sources of external work in level walking and running," *J. Physiol.*, vol. 262, no. 3, pp. 639–657, 1976.

[5] J. R. Montgomery and A. M. Grabowski, "The contributions of ankle, knee and hip joint work to individual leg work change during uphill and downhill walking over a range of speeds," *Roy. Soc. Open Sci.*, vol. 5, no. 8, p. 14, Aug. 2018.

[6] A. Grabowski, C. T. Farley, and R. Kram, "Independent metabolic costs of supporting body weight and accelerating body mass during walking," *J. Appl. Physiol.*, vol. 98, no. 2, pp. 579–583, Feb. 2005.

[7] T. M. Griffin, T. J. Roberts, and R. Kram, "Metabolic cost of generating muscular force in human walking: Insights from load-carrying and speed experiments," *J. Appl. Physiol.*, vol. 95, no. 1, pp. 83–172, 2003.

[8] M. Hao, K. Chen, and C. L. Fu, "Effects of hip torque during step-to-step transition on center-of-mass dynamics during human walking examined with numerical simulation," *J. Biomech.*, vol. 90, no. 1, pp. 33–39, Jun. 2019.

[9] M. Wisse, C. G. Atkeson, and D. K. Kloimwieder, "Swing leg retraction helps biped walking stability," in *Proc. 5th IEEE-RAS Int. Conf. Humanoid Robots*, Dec. 2005, pp. 295–300.

[10] F. Giovacchini *et al.*, "A light-weight active orthosis for hip movement assistance," *Robot. Auton. Syst.*, vol. 73, no. 1, pp. 123–134, Nov. 2015.

[11] H.-J. Lee *et al.*, "A wearable hip assist robot can improve gait function and cardiopulmonary metabolic efficiency in elderly adults," *IEEE Trans. Neural Syst. Rehabil. Eng.*, vol. 25, no. 9, pp. 1549–1557, Sep. 2017.

[12] B. Zhong *et al.*, "Toward gait symmetry enhancement via a cable-driven exoskeleton powered by series elastic actuators," *IEEE Robot. Autom. Lett.*, vol. 7, no. 2, pp. 786–793, Dec. 2021.

[13] T. Zhang, M. Tran, and H. Huang, "Design and experimental verification of hip exoskeleton with balance capacities for walking assistance," *IEEE-ASME Trans. Mechatron.*, vol. 23, no. 1, pp. 274–285, Feb. 2018.

[14] Z. Li *et al.*, "Human-in-the-loop control of a wearable lower limb exoskeleton for stable dynamic walking," *IEEE-ASME Trans. Mechatron.*, vol. 26, no. 5, pp. 2700–2711, Nov. 2021.

[15] B. Chen *et al.*, "Recent developments and challenges of lower extremity exoskeletons," *J. Orthopaedic Transl.*, vol. 5, pp. 26–37, Apr. 2016.

[16] A. J. Young and D. P. Ferris, "State of the art and future directions for lower limb robotic exoskeletons," *IEEE Trans. Neural Syst. Rehabil. Eng.*, vol. 25, no. 2, pp. 171–182, Feb. 2017.

[17] L. X. Chen *et al.*, "A novel lightweight wearable soft exosuit for reducing the metabolic rate and muscle fatigue," *Biosensors*, vol. 11, no. 7, p. 15, Jul. 2021.

[18] S. Jin, N. Iwamoto, K. Hashimoto, and M. Yamamoto, "Experimental evaluation of energy efficiency for a soft wearable robotic suit," *IEEE Trans. Neural Syst. Rehabil. Eng.*, vol. 25, no. 8, pp. 1192–1201, Oct. 2016.

[19] X. Wu, K. Fang, C. Chen, and Y. Zhang, "Development of a lower limb multi-joint assistance soft exosuit," *Sci. China Inf. Sci.*, vol. 63, no. 7, p. 3, May 2020.

[20] Y. Ding *et al.*, "Biomechanical and physiological evaluation of multi-joint assistance with soft exosuits," *IEEE Trans. Neural Syst. Rehabil. Eng.*, vol. 25, no. 2, pp. 119–130, Feb. 2017.

[21] G. Lee *et al.*, "Reducing the metabolic cost of running with a tethered soft exosuit," *Sci. Robot.*, vol. 2, no. 6, p. 6708, May 2017.

[22] J. Kim *et al.*, "Reducing the metabolic rate of walking and running with a versatile, portable exosuit," *Sci.*, vol. 365, no. 6454, pp. 668–672, Aug. 2019.

[23] S. Guo, Q. Xiang, K. Hashimoto, and S. Jin, "Assistive force of a belt-type hip assist suit for lifting the swing leg during walking," in *Proc. IEEE Int. Conf. Robot. Autom. (ICRA)*, May 2020, pp. 4841–4847.

[24] P. J. Mansfield and D. A. Neumann, "Fundamentals of human gait," in *Essentials of Kinesiology for the Physical Therapist Assistant*. St. Louis, MO, USA: Mosby, 2011, ch. 12, pp. 351–367.

[25] S. A. Chvatal and L. H. Ting, "Common muscle synergies for balance and walking," *Frontiers Comput. Neurosci.*, vol. 7, p. 48, May 2013.

[26] I. Kang, H. Hsu, and A. Young, "The effect of hip assistance levels on human energetic cost using robotic hip exoskeletons," *IEEE Robot. Autom. Lett.*, vol. 4, no. 2, pp. 430–437, Apr. 2019.
[27] C. M. Thalman *et al.*, "A soft robotic hip exosuit (SR-HExo) to assist hip flexion and extension during human locomotion," in *Proc. IEEE Int. Conf. Intell. Rob. Sys.*, Sep. 2021, pp. 5060–5066.
[28] Q. Chen, S. Guo, L. Sun, Q. Liu, and S. Jin, "Inertial measurement unit-based optimization control of a soft exosuit for hip extension and flexion assistance," *J. Mech. Robot.*, vol. 13, no. 2, p. 10, Apr. 2021.
[29] R. Margaria, "Positive and negative work performances and their efficiencies in human locomotion," *Internationale Zeitschrift für Angewandte Physiologie Einschließlich Arbeitsphysiologie*, vol. 25, no. 4, pp. 339–351, May 1968.
[30] P. DeVita, J. Helseth, and T. Hortobagyi, "Muscles do more positive than negative work in human locomotion," *J. Experim. Biol.*, vol. 210, no. 19, pp. 3361–3373, Oct. 2007.
[31] U. Trinler, H. Schwameder, R. Baker, and N. Alexander, "Muscle force estimation in clinical gait analysis using AnyBody and OpenSim," *J. Biomechanics*, vol. 86, pp. 55–63, Mar. 2019.
[32] A. T. Asbeck, S. M. M. D. Rossi, K. G. Holt, and C. J. Walsh, "A biologically inspired soft exosuit for walking assistance," *Int. J. Robot. Res.*, vol. 34, no. 6, pp. 744–762, Mar. 2015.
[33] (2015). *SENIAM*. [Online]. Available: http://www.seniam.org/
[34] N. Zuntz, "Ueber die bedeutung der verschiedenen Nährstoffe als erzeuger der muskelkraft," *Archiv für die Gesamte Physiologie des Menschen und der Tiere*, vol. 83, nos. 10–12, pp. 557–571, Feb. 1901.
[35] E. Fuglei and N. A. Oritsland, "Body composition, resting and running metabolic rates, and net cost of running in rats during starvation," *Acta Physiol. Scand.*, vol. 165, no. 2, pp. 203–210, 1999.
[36] J. McDaniel *et al.*, "Determinants of metabolic cost during submaximal cycling," *J. Appl. Physiol.*, vol. 93, no. 3, pp. 823–828, 2002.
[37] V. L. Katch, W. D. McArdle, and F. I. Katch, "Energy transfer," in *Essentials of Exercise Physiology*, vol. 3, 4th ed. Philadelphia, PA, USA: Wolters Kluwer, 2011, ch. 5, pp. 246–248.
[38] R. C. Bishop, "Metaphysical and epistemological issues in complex systems," in *Philosophy of Complex Systems* (Handbook of the Philosophy of Science), C. Hooker, Ed. Amsterdam, The Netherlands: Elsevier, 2011, pp. 105–136.
[39] S van Sint Jan, "Color atlas of skeletal landmark definitions," in *Guidelines for Reproducible Manual and Virtual Palpations*. New York, NY, USA: Churchill Livingstone, 2009, pp. 234–235.
[40] W. Wang, Y. Xiao, S. Yue, N. Wei, and K. Li, "Analysis of center of mass acceleration and muscle activation in hemiplegic paralysis during quiet standing," *PLoS ONE*, vol. 14, no. 12, Dec. 2019, Art. no. e0226944.
[41] D. A. Winter, "Energy generation and absorption at the ankle and knee during fast, natural, and slow cadences," *Clin. Orthopaedics Rel. Res.*, vol. 175, pp. 147–154, May 1983.
[42] F. A. Panizzolo *et al.*, "A biologically-inspired multi-joint soft exosuit that can reduce the energy cost of loaded walking," *J. Neuroeng. Rehabil.*, vol. 13, no. 1, p. 43, May 2016.
[43] H. Barazesh and M. A. Sharbafi, "A biarticular passive exosuit to support balance control can reduce metabolic cost of walking," *Bioinspiration Biomimetics*, vol. 15, no. 3, May 2020, Art. no. 036009.
[44] F. A. Panizzolo, C. Bolgiani, L. Di Liddo, E. Annese, and G. Marcolin, "Reducing the energy cost of walking in older adults using a passive hip flexion device," *J. NeuroEng. Rehabil.*, vol. 16, no. 1, pp. 117–124, Oct. 2019.
[45] T. Zhou, C. Xiong, J. Zhang, D. Hu, W. Chen, and X. Huang, "Reducing the metabolic energy of walking and running using an unpowered hip exoskeleton," *J. NeuroEng. Rehabil.*, vol. 18, no. 1, p. 95, Jun. 2021.
[46] S. H. Collins, M. B. Wiggin, and G. S. Sawicki, "Reducing the energy cost of human walking using an unpowered exoskeleton," *Nature*, vol. 522, no. 7555, pp. 212–215, Jun. 2015.
[47] S. Lee *et al.*, "Autonomous multi-joint soft exosuit with augmentation-power-based control parameter tuning reduces energy cost of loaded walking," *J. NeuroEng. Rehabil.*, vol. 15, no. 1, p. 66, Jul. 2018.
[48] J. E. A. Bertram, "Locomotion: Why we walk the way we walk," *Current Biol.*, vol. 25, no. 18, pp. R795–R797, Sep. 2015.
[49] J. C. Selinger, S. M. O'Connor, J. D. Wong, and J. M. Donelan, "Humans can continuously optimize energetic cost during walking," *Current Biol.*, vol. 25, no. 18, pp. 2452–2456, Sep. 2015.
[50] D. Lee *et al.*, "Biomechanical comparison of assistance strategies using a bilateral robotic knee exoskeleton," *IEEE Trans. Biomed. Eng.*, vol. 68, no. 9, pp. 2870–2879, Sep. 2021.
[51] H. Park, J. Lan, J. Zhang, K. Chen, and C. Fu, "Design of a soft wearable device for hip and knee extension assistance," in *Proc. 5th Int. Conf. Control, Autom. Robot. (ICCAR)*, Apr. 2019, pp. 798–801.
[52] D. J. Farris and G. S. Sawicki, "The mechanics and energetics of human walking and running: A joint level perspective," *J. Roy. Soc. Interface*, vol. 9, no. 66, pp. 110–118, Jan. 2012.
[53] F. Asano and Z.-W. Luo, "Efficient dynamic bipedal walking using effects of semicircular feet," *Robotica*, vol. 29, no. 3, pp. 351–365, May 2011.
[54] K. E. Gordon, D. P. Ferris, and A. D. Kuo, "Metabolic and mechanical energy costs of reducing vertical center of mass movement during gait," *Arch. Phys. Med. Rehabil.*, vol. 90, no. 1, pp. 136–144, Jan. 2009.
[55] Y. Fan, "Dynamic principle of center of mass in human walking," *Brit. Biotechnol. J.*, vol. 3, no. 4, pp. 524–544, Jan. 2013.